Electronic Supplementary Material (ESI) for Catalysis Science & Technology.

Heterogeneous Self-Supported Dirhodium (II) Catalysts with High Catalytic Efficiency in Cyclopropanation – A structural study

Jiquan Liu[a], Claudia Fasel[b], Pedro Braga-Groszewicz[a], Niels Rothermel[a], Aany Sofia Lilly Thankamony[a], Grit Sauer[a], Yeping Xu[a*], Torsten Gutmann[a*], Gerd Buntkowsky[a*]

[a] Eduard-Zintl-Institute for Inorganic Chemistry and Physical Chemistry, Technical University Darmstadt, Alarich-Weiss-Straße 8, D-64287 Darmstadt, Germany
[b] FB Material- und Geowissenschaften, Technical University Darmstadt, Alarich-Weiss-Strasse 2, 64287 Darmstadt, Germany
E-mail: Gerd.Buntkowsky@chemie.tu-darmstadt.de; gutmann@chemie.tu-darmstadt.de; Xu@ chemie.tu-darmstadt.de

Contents

1. Schematic drawing of dirhodium complexes 2
2. XPS 3
3. ^{19}F MAS NMR 4
4. TG-DTA 5
5. ATR-IR 6
6. ^{13}C CP MAS NMR 7
7. DFT calculation 8
8. Liquid ^{19}F NMR 10
9. UV-vis 11
10. EPR 12
11. Catalytic test 13
12. ICP-OES 14
13. References 15

1. Schematic drawing of dirhodium complexes

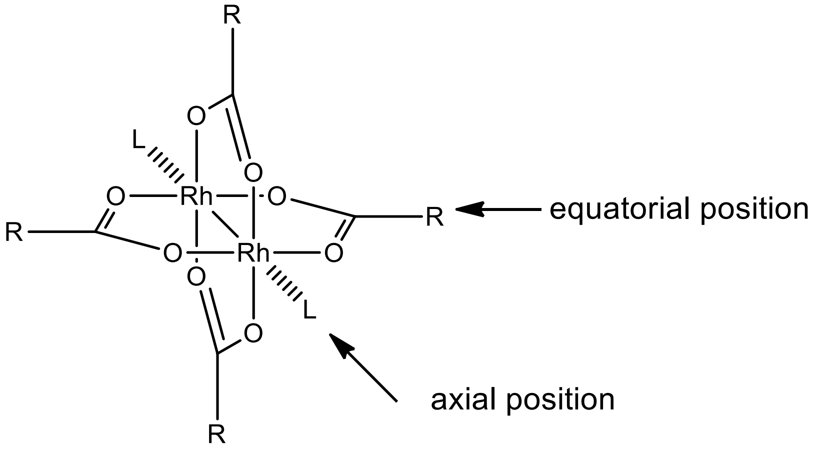

R= CH_3 or CF_3
L = axial ligand
catalytic sites are at axial positons

Scheme S1. Schematic drawing of dirhodium complexes.

The dirhodium complexes possess a paddlewheel structure including a Rh-Rh single bond with four carboxylate groups at equatorial positions, such as $Rh_2(TFA)_4$ or $Rh_2(OAc)_4$ as illustrated in **Scheme S1**. Solvent or substrate molecule can coordinate at axial positions which are catalytic sites.[1]

2. XPS

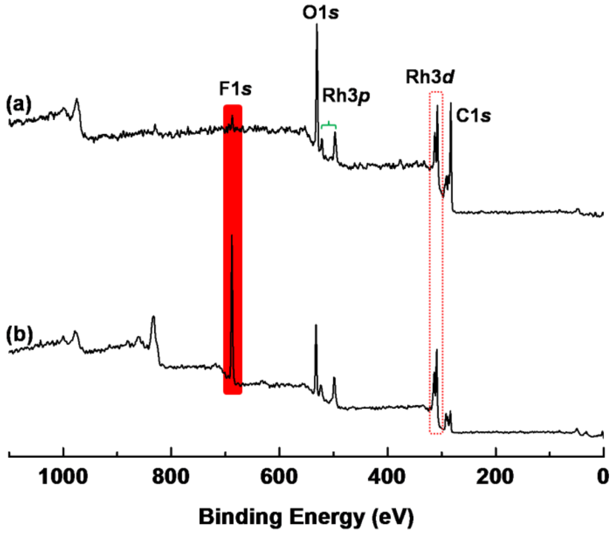

Figure S1. XPS of Rh_2-bdc(Tf) (a), and neat $Rh_2(TFA)_4$ complex (b) in wide scan mode.

3. ^{19}F MAS NMR

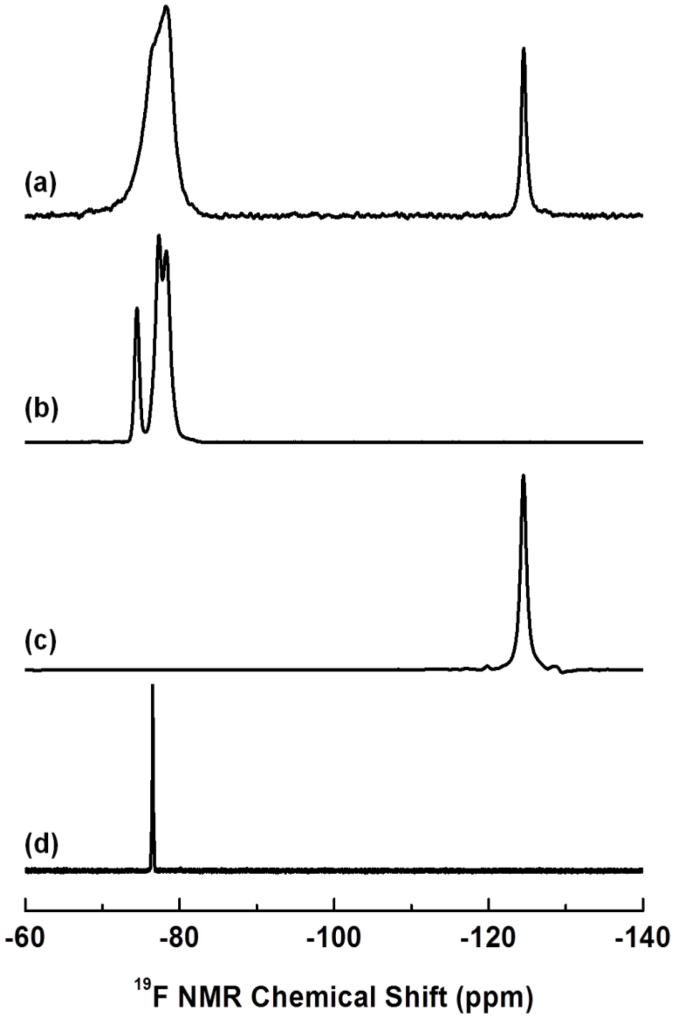

Figure S2. ^{19}F MAS solid-state NMR spectra of Rh_2-bdc(Tf) (a), $Rh_2(TFA)_4$ (b) and PTFE (c) as well as static spectrum of trifluoroacetic acid employed as reference (d).

In the ^{19}F MAS NMR spectrum of Rh_2-bdc(Tf) (Figure S2a), two signals are observed (-76 ppm (broad) and -125 ppm (sharp)). The signal at ca. -76 ppm refers to trifluoroacetate, since it appears in the same region as trifluoroacetate in $Rh_2(TFA)_4$ (Figure S2b) and trifluoroacetic acid (Figure S2d). The signal located at -125 ppm (Figure S2a) corresponds to polytetrafluoroethylene (PTFE) (Figure S2c). The presence of this signal in the coordination polymer sample may be attributed to small amounts of material scraped from the magnetic stirrer employed during the synthesis.

4. TG-DTA

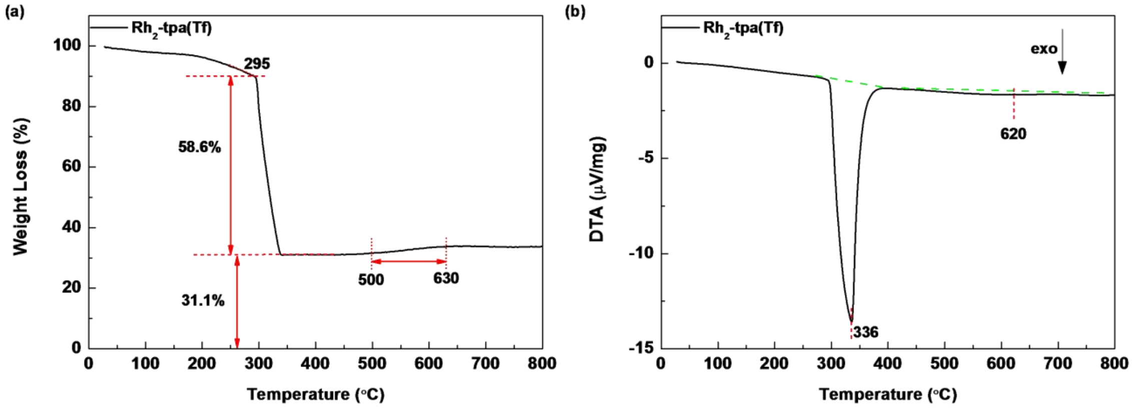

Figure S3. TG (a) and DTA (b) curves of Rh_2-bdc(Tf) measured under oxygen atmosphere.

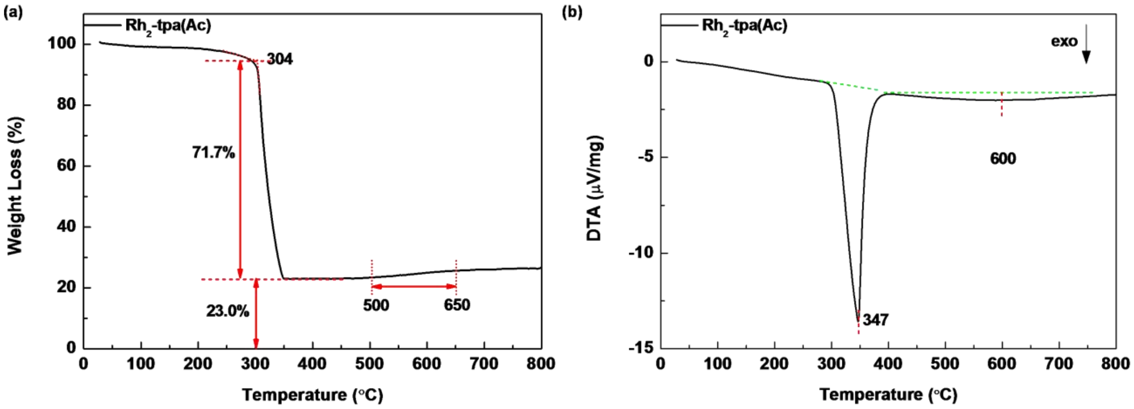

Figure S4. TG (a) and DTA (b) curves of Rh_2-bdc(Ac) measured under oxygen atmosphere.

According to TG and DTA data, the dried Rh_2-bdc(Tf) and Rh_2-bdc(Ac) show thermal stability up to 200 °C in O_2 atmosphere, which is similar to the results obtained by Kaskel et al.[2] For both samples, the mass rise between 500 °C to 650 °C in the TG curves combined with broad exothermic peaks (centered at 620 or 600 °C) in the DTA curves indicate the formation of rhodium oxides. Based on the residual mass at 350 °C, the rhodium contents for both samples are approximated as 31.1% and 23.0% for Rh_2-bdc(Tf) and Rh_2-bdc(Ac), respectively.

5. ATR-IR

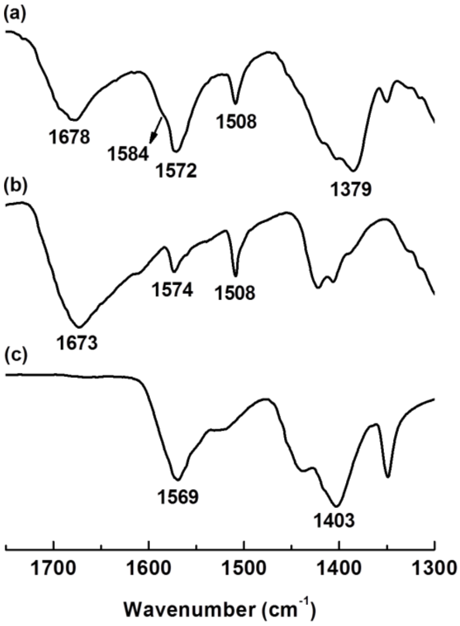

Figure S5. ATR-IR spectra of Rh_2-bdc(Ac) (a), neat BDC (b) and $Rh_2(OAc)_4$ complex (c).

6. ^{13}C CP MAS NMR

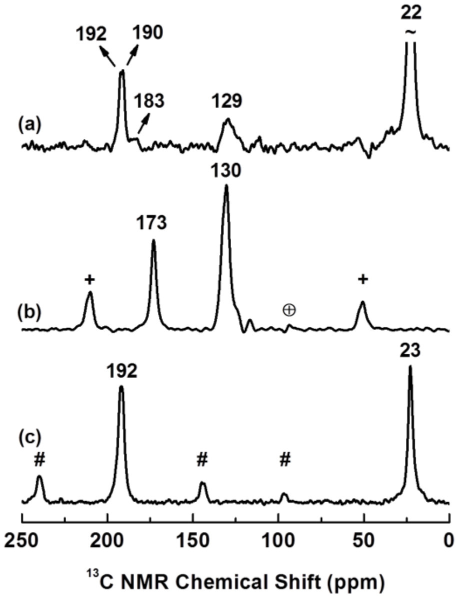

Figure S6. ^{13}C CP MAS NMR spectra of Rh_2-bdc(Ac) (a) at 7 T and 6 kHz spinning, neat BDC (b) at 7 T and 6 kHz spinning, and $Rh_2(OAc)_4$ complex (c) at 11.7 T field and 6 kHz spinning.

Notes: Signals marked with + and ⊕ are spinning sidebands of the carboxyl and phenyl group at 173 and 130 ppm of BDC, respectively. Signals marked with # are spinning side bands of the carboxyl group at 192 ppm of $Rh_2(OAc)_4$.

7. DFT calculation

DFT calculations were performed with the ORCA[3] program system, employing model structures that are based on the crystal structure of $Rh_2(OAc)_4(H_2O)_2$.[4] The TFA ligands were introduced by replacing the methyl hydrogen atoms by fluorine prior to the geometry optimization, which was performed with Becke's three-parameter functional[5] along with the Lee-Yang-Parr correlation functional (B3LYP)[6], and Poples double-ζ basis set 6-31G(d,p)[7] combining d- and p-polarization functions. In all calculations the core electrons of Rh were replaced by a relativistic effective core potential (ECP) developed by the Stuttgart group.[8]
The ^{19}F magnetic shieldings were calculated at the B3LYP level of theory, and the triple-ζ basis set 6-311++G(3df,3dp) including four sets of polarization functions and additional diffuse functions on all atoms.[7, 9]

Table S1. Model compounds employed for DFT calculations, and corresponding magnetic shieldings of the florins in these complexes.

compound	model	magnetic shielding (ppm)
$Rh_2(TFA)(OAc)_3$	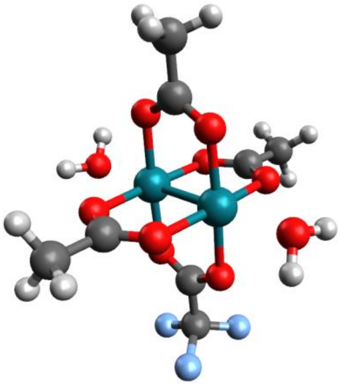	215.67
cis-$Rh_2(TFA)_2(OAc)_2$	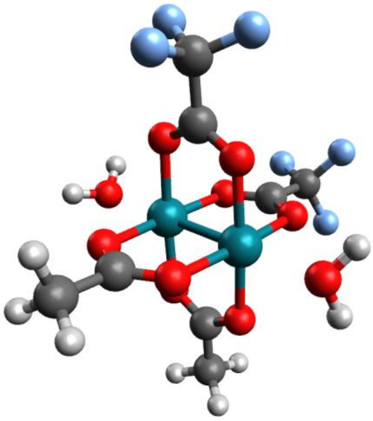	215.97

trans- $Rh_2(TFA)_2(OAc)_2$	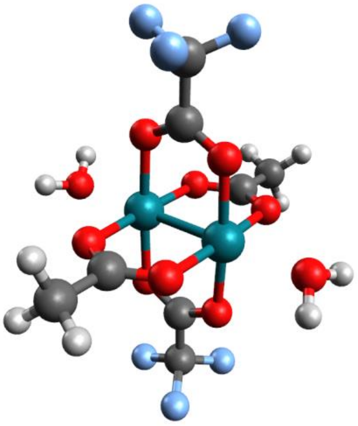	208.87
$Rh_2(TFA)_3(OAc)$	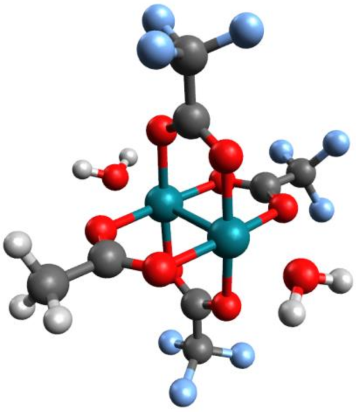	*trans*-Tf/Tf 209.97 *trans*-Tf/Ac 216.87

8. Liquid ^{19}F NMR

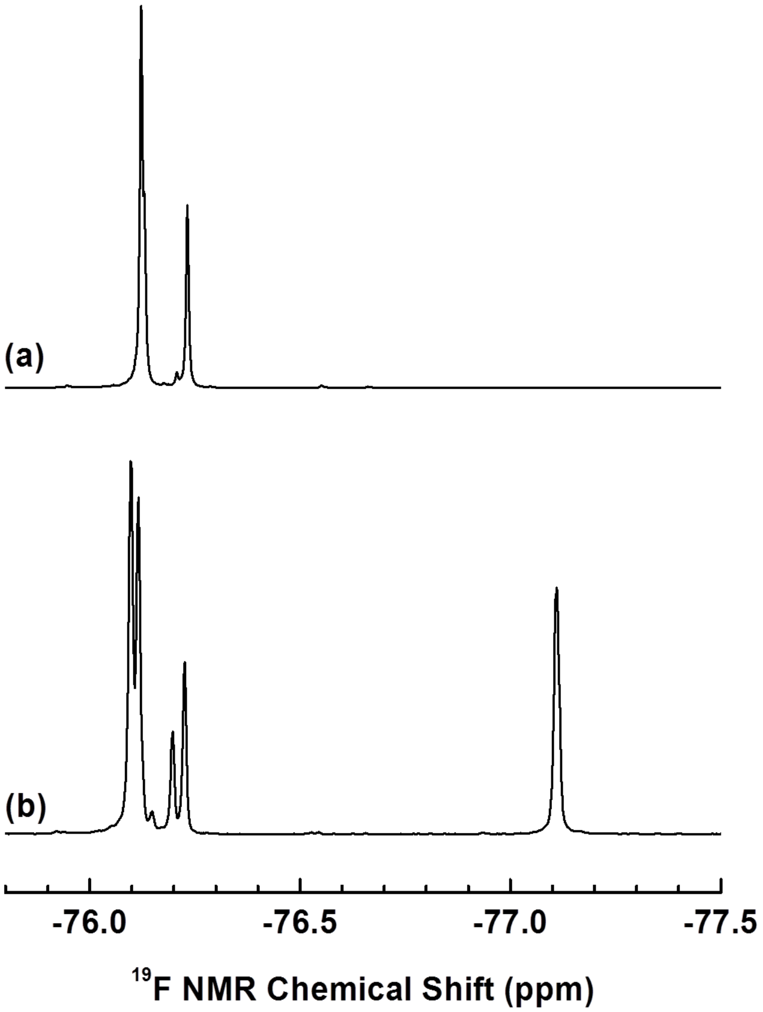

Figure S7. ^{19}F solution NMR spectra of neat $Rh_2(TFA)_4$ in EtOAc (a), and $Rh_2(TFA)_4$ + HOAc in EtOAc after 1h of reaction (b).

Note: To perform the reaction of $Rh_2(TFA)_4$ and HOAc, 0.0600 g (0.09 mmol) $Rh_2(TFA)_4$ was dissolved in 20 mL EtOAc. Then, 0.22 g (3.6 mmol) HOAc was added into the solution. Thereafter, the reaction was performed at 95 °C and a liquid sample was picked after 1 h of reaction. All spectra were recorded in solution adding 3 drops of CD_2Cl_2.

For neat $Rh_2(TFA)_4$, the ^{19}F NMR signals are located at ca. -76.2 ppm. After ligand substitution, another peak at ca. -77.1 ppm appeared, which clearly illustrates that ligand exchange occurs and that the fluorine chemical environment changes. The peak at high field (77.1 ppm) most probably refers to trifluoroacetate groups which contain an OAc ligand in *trans*-position.

This observation in ^{19}F liquid state NMR corroborates the results from the DFT calculation, and may help to understand the broad peak containing two signals in the ^{19}F solid-state NMR spectrum of Rh_2-bdc(Tf).

9. UV-vis

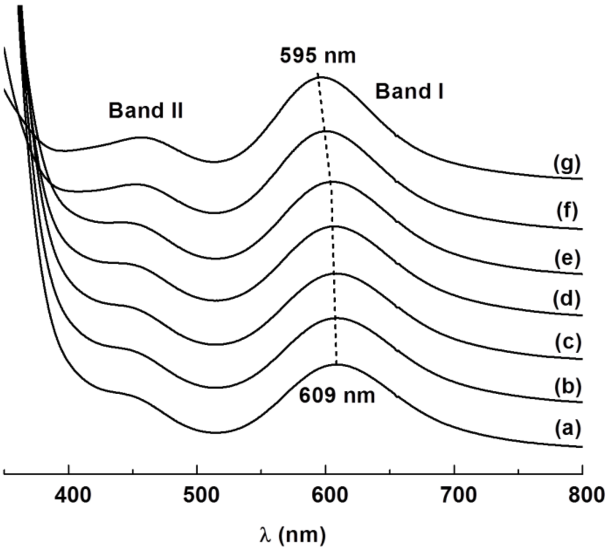

Figure S8. UV-vis spectra of mixtures of $Rh_2(TFA)_4$ /ethyl acetate with molar ratios of 1/0 (a), 1/1 (b), 1/2 (c), 1/6 (d), 1/10(e), 1/1800 (f) and 1/3600 (g).

Note: Liquid samples were recorded on a TIDAS 100 MCS spectrometer (J&M Analtik AG). For each measurement, a solution of 0.6 mL CH_2Cl_2 containing a $Rh_2(TFA)_4$ concentration of 0.94 mmol·L^{-1} was introduced into a 1 mL quartz cuvette (10.00 mm QS Hellma Analytics). Various amounts of ethyl acetate to reach the appropriate $Rh_2(TFA)_4$ /ethyl acetate ratios were added via syringe.

The location of band I is sensitive to the axial coordination environment, which shifts from 603 nm (in acetone) to 587 nm (in H_2O, O coordinating at *ax* position) and then to 552 nm (in acetonitrile, N coordinating at *ax* position).[10] According to the ^{13}C CP MAS NMR, ethyl acetate exists as guest molecule in Rh_2-bdc(Tf). To figure out the effect of ethyl acetate, the UV-vis adsorption of $Rh_2(TFA)_4$ in dichloromethane containing different amounts of the ethyl acetate were recorded (Figure S6). The spectra show that a blue shift is obtained when larger amounts of ethyl acetate are present in the $Rh_2(TFA)_4$-ethyl acetate solution.

For the vacuum dried Rh_2-bdc(Tf) sample, the location of band I at 625 nm reveals that the axial position of the dirhodium moieties may be vacant or occupied by limited amounts of ethyl acetate. This would explain the red shift of this band compared to liquid samples containing *ax*-coordinating ethyl acetate ligands.

10. EPR

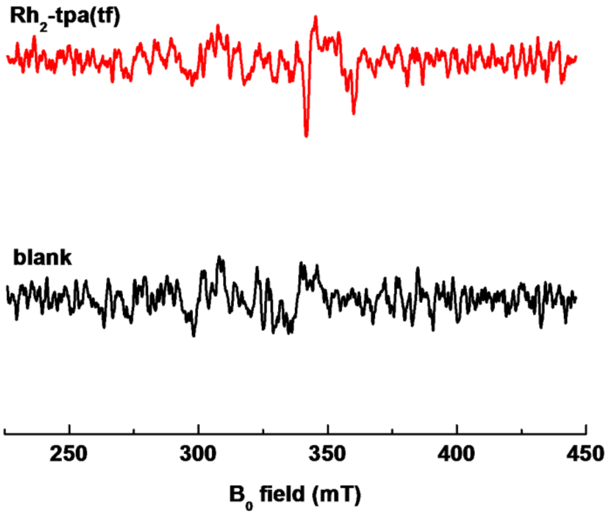

Figure S9. EPR spectra of Rh$_2$-bdc(Tf) and blank tube.

The EPR spectrum for Rh$_2$-bdc(Tf) was recorded on an EPR Miniscope MS-400 (Magnettech) equipped with a FC-400 resonator. The measurement was carried out at 9.43 GHz at room temperature employing 0.4 mT modulation amplitude at 100 kHz modulation frequency**.** The sample was measured under 3.5 dB microwave attenuation with 30 s sweep time and 4096 points. The control measurement for blank tube was performed under the same condition.

Since for both samples no significant EPR signals were observed it can be concluded that no free Rh^{2+} species are present in the sample, or they are below the detection limit of the EPR.

11. Catalytic test

Table S2. Fitting results of Rh_2-bdc(Tf) and $Rh_2(TFA)_4$[a].

	Rh_2-bdc(Tf)		$Rh_2(TFA)_4$	
	Value	Standard Error	Value	Standard Error
y_0	80.01929	3.52482	65.65962	1.29524
A	-76.33959	4.75851	-65.24289	2.15078
t	3.94732	0.67488	3.04935	0.23853
Adj. R-Square	0.97363	-	0.99463	-
k[b]	0.25	0.04	0.33	0.03

Note: [a] The yield of Rh_2-bdc(Tf) and $Rh_2(TFA)_4$ was fitted according to equation $y = A*\exp(-x/t) + y_0$ assuming a first order reaction. [b] The initial rate constant is calculated according to $k = 1/t$.

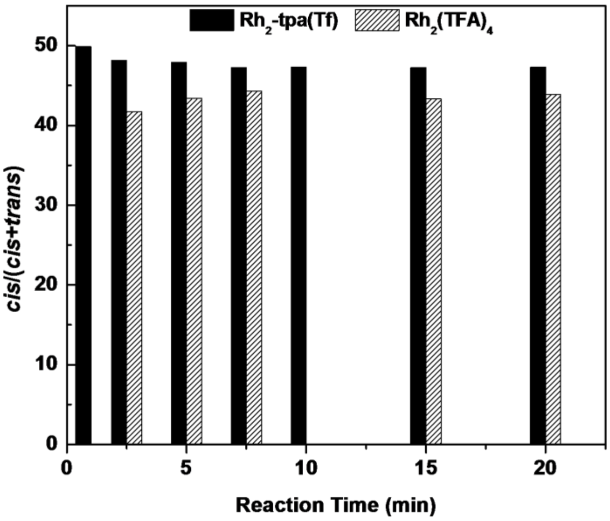

Figure S10. Diastereoselectivity in form of *cis*/(*cis*+*trans*) plot versus reaction time for Rh_2-bdc(Tf) (a) and neat $Rh_2(TFA)_4$ complex (b).

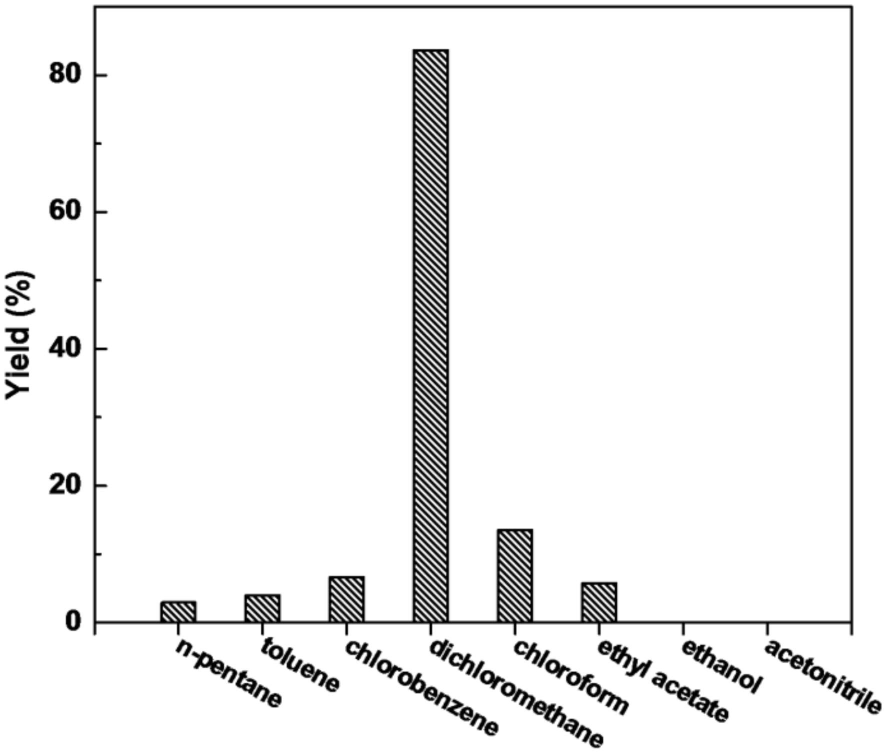

Figure S11. Yield of products received with the Rh_2-bdc(Tf) catalyst employing various solvents

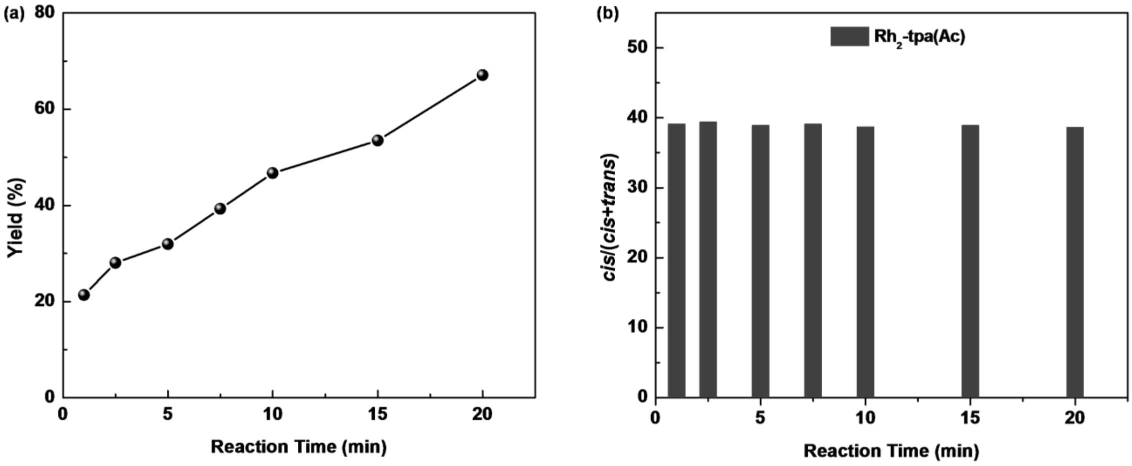

Figure S12. Yield of products (a) and diastereoselectivity in form of *cis*/(*cis*+*trans*) plot versus reaction time for Rh_2-bdc(Ac) (b).

12. ICP-OES

The filtrated solution from the leaching test (13 mL) was collected for ICP-OES measurement to analyze the residual rhodium fraction. After evaporation of the solvent, the organic matrix was removed by heating the sample at 650 °C for 4 h, and the residue was dissolved in aqua regia at 50 °C for 24 h. Note that aqua regia was prepared by mixing 3 mL HCl (≥ 37%) and 1 mL HNO_3 (≥ 69.0%). Both acids were employed with high purity grade for trace analysis (TraceSELECT®, FLUKA).

After dilution with deionized water (1 mL aqua regia in 10 mL aqueous solution, pH: 1.0-1.5), a volume of 10 mL of the analyte was obtained. Finally, the solution was filtered via a SPARTAN® syringe filter (0.2 µm pore size). The following analysis was performed by the AZBA GmbH, Berlin.

Diluted aqua regia (1 mL aqua regia in 10 mL aqueous solution, pH: 1.0-1.5) was employed as blank sample (see Probe 1 in Table S3).

Table S3. ICP-OES for blank solution (Probe 1) and leaching solution (Probe 2)

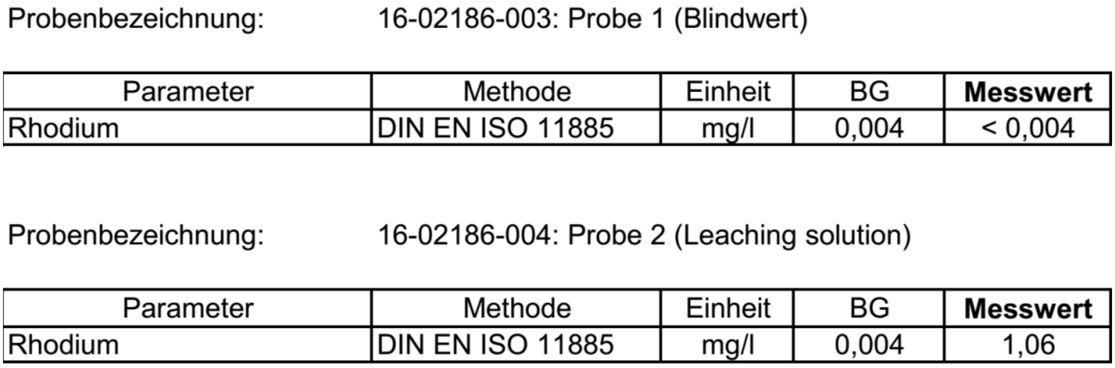

Probenbezeichnung: 16-02186-003: Probe 1 (Blindwert)

Parameter	Methode	Einheit	BG	**Messwert**
Rhodium	DIN EN ISO 11885	mg/l	0,004	< 0,004

Probenbezeichnung: 16-02186-004: Probe 2 (Leaching solution)

Parameter	Methode	Einheit	BG	**Messwert**
Rhodium	DIN EN ISO 11885	mg/l	0,004	1,06

The Rh concentration in the tested solution (10 mL) was determined to be 1.06 ppm.

Finally, the rhodium content in the reaction solution was calculated as follow:

$$\mathrm{Rh\%(reaction\ solution)} = 1.06\mathrm{ppm} \times \frac{10\mathrm{mL}}{13\mathrm{mL}} = 0.815\ \mathrm{ppm}$$

13. References

1. (a) Chifotides, H.; Dunbar, K., Rhodium Compounds. In *Multiple Bonds Between Metal Atoms*, Cotton, F. A.; Murillo, C.; Walton, R., Eds. Springer US: 2005; pp 465-589; (b) Boyar, E. B.; Robinson, S. D., *Coord. Chem. Rev.* **1983,** *50* (1–2), 109-208.
2. Nickerl, G.; Stoeck, U.; Burkhardt, U.; Senkovska, I.; Kaskel, S., *J. Mater. Chem. A* **2014,** *2* (1), 144-148.
3. Neese, F., *Wiley Interdisciplinary Reviews: Computational Molecular Science* **2012,** *2* (1), 73-78.
4. Cotton, F. A.; DeBoer, B. G.; LaPrade, M. D.; Pipal, J. R.; Ucko, D. A., *Acta Crystallographica Section B* **1971,** *27* (8), 1664-1671.
5. (a) Becke, A. D., *The Journal of Chemical Physics* **1993,** *98* (7), 5648-5652; (b) Becke, A. D., *The Journal of Chemical Physics* **1993,** *98* (2), 1372-1377.
6. Lee, C.; Yang, W.; Parr, R. G., *Physical Review B* **1988,** *37* (2), 785-789.
7. (a) Hehre, W. J.; Ditchfield, R.; Pople, J. A., *The Journal of Chemical Physics* **1972,** *56* (5), 2257-2261; (b) Dill, J. D.; Pople, J. A., *The Journal of Chemical Physics* **1975,** *62* (7), 2921-2923.
8. Peterson, K. A.; Figgen, D.; Dolg, M.; Stoll, H., *The Journal of Chemical Physics* **2007,** *126* (12),

124101.

9. (a) Krishnan, R.; Binkley, J. S.; Seeger, R.; Pople, J. A., *The Journal of Chemical Physics* **1980,** *72* (1), 650-654; (b) Clark, T.; Chandrasekhar, J.; Spitznagel, G. W.; Schleyer, P. V. R., *J. Comput. Chem.* **1983,** *4* (3), 294-301; (c) Frisch, M. J.; Pople, J. A.; Binkley, J. S., *The Journal of Chemical Physics* **1984,** *80* (7), 3265-3269.

10. Johnson, S. A.; Hunt, H. R.; Neumann, H. M., *Inorg. Chem.* **1963,** *2* (5), 960-962.